NAVAL POSTGRADUATE SCHOOL
Monterey, California

THESIS

THE EFFECT OF HEAT TREATMENT AND CYCLIC STRAIN AMPLITUDE ON THE DAMPING PROPERTIES OF IRON-CHROMIUM BASED ALLOYS

by

James L. Childs, Jr.

June 1988

Thesis Advisor: Jeff Perkins

Approved for public release; distribution is unlimited

REPORT DOCUMENTATION PAGE

1a. REPORT SECURITY CLASSIFICATION UNCLASSIFIED	1b RESTRICTIVE MARKINGS
2a. SECURITY CLASSIFICATION AUTHORITY	3 DISTRIBUTION/AVAILABILITY OF REPORT Approved for public release; distribution is unlimited
2b DECLASSIFICATION/DOWNGRADING SCHEDULE	
4. PERFORMING ORGANIZATION REPORT NUMBER(S)	5 MONITORING ORGANIZATION REPORT NUMBER(S)
6a NAME OF PERFORMING ORGANIZATION Naval Postgraduate School 6b OFFICE SYMBOL (*If applicable*) Code 69	7a. NAME OF MONITORING ORGANIZATION Naval Postgraduate School
6c. ADDRESS (*City, State, and ZIP Code*) Monterey, California 93943-5000	7b. ADDRESS (*City, State, and ZIP Code*) Monterey, California 93943-5000
8a NAME OF FUNDING SPONSORING ORGANIZATION 8b OFFICE SYMBOL (*If applicable*)	9. PROCUREMENT INSTRUMENT IDENTIFICATION NUMBER
8c. ADDRESS (*City, State, and ZIP Code*)	10. SOURCE OF FUNDING NUMBERS PROGRAM ELEMENT NO. / PROJECT NO. / TASK NO / WORK UNIT ACCESSION NO.

11 TITLE (*Include Security Classification*)
THE EFFECT OF HEAT TREATMENT AND CYCLIC STRAIN AMPLITUDE ON THE DAMPING PROPERTIES OF IRON-CHROMIUM BASED ALLOYS

12. PERSONAL AUTHOR(S)
Childs, James L. Jr.

13a. TYPE OF REPORT	13b TIME COVERED	14. DATE OF REPORT (*Year, Month, Day*)	15 PAGE COUNT
Master's Thesis	FROM _____ TO _____	1988, June	66

16 SUPPLEMENTARY NOTATION
The views expressed in this thesis are those of the author and do not reflect the official policy or positions of the Department of Defense or the United States Government.

17 COSATI CODES			18 SUBJECT TERMS (*Continue on reverse if necessary and identify by block number*)
FIELD	GROUP	SUB-GROUP	
			Cyclic Strain Amplitude; Damping Properties; Iron-Chromium Based Alloys, Heat Treatment, Molybdenum Aluminum, THESES, (DES)

19 ABSTRACT (*Continue on reverse if necessary and identify by block number*)

Fe-Cr-Al and Fe-Cr-Mo alloys are being studied for their high damping characteristics and possible utility to the Navy in the noise reduction and vibration control of shipboard machinery systems. This research studied the dependence of damping in these alloys on heat treatment and cyclic strain amplitude. Tensile specimens annealed at 900 C and 1100 C were subjected to cyclic axial loading at low strain levels on an MTS mechanical testing system, generating load-displacement hysteresis loops at various frequencies. These hysteresis loops were analyzed to determine the damping response at various levels of loading. Damping capacity is found to be dependent on both strain amplitude and frequency. A comparison is made between these results and previous work which evaluated the strain dependence of damping in these alloys using more conventional experimental methods. Keywords: (DES)

20 DISTRIBUTION/AVAILABILITY OF ABSTRACT	21. ABSTRACT SECURITY CLASSIFICATION
☒ UNCLASSIFIED/UNLIMITED ☐ SAME AS RPT ☐ DTIC USERS	Unclassified
22a NAME OF RESPONSIBLE INDIVIDUAL Prof. Jeff Perkins	22b TELEPHONE (*Include Area Code*) (408) 646-2216 22c. OFFICE SYMBOL Code 69Ps

Approved for public release; distribution is unlimited

The Effect of Heat Treatment and Cyclic Strain Amplitude on the Damping Properties of Iron-Chromium Based Alloys

by

James L. Childs, Jr.
Lieutenant, United States Navy
B.S., M.I.T., 1982

Submitted in partial fulfillment of the requirements for the degree of

MASTER OF SCIENCE IN MECHANICAL ENGINEERING

from the

NAVAL POSTGRADUATE SCHOOL
June 1988

Author: _____
James L. Childs, Jr.

Approved by: _____
Jeff Perkins, Thesis Advisor

_____
Anthony J. Healey, Chairman
Department of Mechanical Engineering

_____
Gordon E. Schacher,
Dean of Science and Engineering

ABSTRACT

Fe-Cr-Al and Fe-Cr-Mo alloys are being studied for their high damping characteristics and possible utility to the Navy in the noise reduction and vibration control of shipboard machinery systems. This research studied the dependence of damping in these alloys on heat treatment and cyclic strain amplitude. Tensile specimens annealed at 900 C and 1100 C were subjected to cyclic axial loading at low strain levels on an MTS mechanical testing system, generating load-displacement hysteresis loops at various frequencies. These hysteresis loops were analyzed to determine the damping response at various levels of loading. Damping capacity is found to be dependent on both strain amplitude and frequency. A comparison is made between these results and previous work which evaluated the strain dependence of damping in these alloys using more conventional experimental methods.

TABLE OF CONTENTS

LIST OF FIGURES

I. INTRODUCTION

A. GENERAL

All dynamic mechanical systems produce noise and vibration to some extent. This is undesirable in a number of respects Continuous, large-amplitude vibrations can impair the performance and ultimately shorten the service life of system components. High noise generation from machinery can cause hearing loss to operating personnel. Underwater acoustic emissions from the propulsion plant noise of Naval vessels may increase their vulnerability to detection by enemy sensors. For all of these reasons the Navy has a continuing interest in all methods of reducing the noise and vibration produced by its shipboard mechanical systems.

Schetky and Perkins [Ref. 1] list three possible techniques for noise and vibration control:

1. Isolate mechanical sources from surfaces which radiate transmitted energy.
2. Dissipate energy within the machinery structure through the use of absorbing pads, rubber insulation, resilient mounts, etc.
3. Attenuate vibrational energy through the use of energy-absorbing (i.e., high damping) materials.

The first two methods take up space and add weight, respectively. Thus the Navy has undertaken research, of which the present research is a part, in an effort to design

"quiet" alloys which possess, along with the required engineering properties, high internal damping characteristics.

B. BACKGROUND

All materials will damp vibration to some extent; this is a property reflecting an excited component's ability to attenuate vibrational energy. However, most common engineering materials have very low damping capacities. For example, Reference 2 indicates that the specific damping capacity (SDC) of most steel and aluminum alloys suitable for structural applications is well under 10 percent at room temperature. Alloy systems in which high damping capacity (SDC over 20 percent) has been observed include those in the Cu-Mn, Cu-Al-Ni, Cu-Zn-Al, Ti-Ni, Fe-Cr-Al and Fe-Cr-Mo systems. The present research studied certain iron-chromium based high damping alloys in which the Navy expressed interest in terms of possible application to shipboard mechanical systems.

Reference 3 presents several mathematical models for materials undergoing forced vibration. For the general case of a sinusoidally excited structure, the Kelvin-Voigt single-degree of freedom model is the simplest one which can still be considered to represent a real mechanical situation. The differential equation for this model is:

$$m\ddot{x} + c\dot{x} + kx = F\exp(iwt) \qquad (1)$$

where:

m = mass

c = viscous damping coefficient

k = elastic spring constant, or stiffness

x = displacement of the system

F = exciting force amplitude

$Fexp(iwt)$ = a complex, time-dependent forcing function

w = excitation frequency

$\ddot{x}$ and $\dot{x}$ = first and second time derivatives of displacement.

The steady state solution to this equation is:

$$x(t) = Xexp(i(wt - \phi) = Fexp(iwt)/((k - mw^2) + iwc) \quad (2)$$

where:

X = displacement amplitude

ϕ = phase angle between the displacement response and the input excitation.

The viscous damping coefficient can be represented as:

$$c = 2mzw(n) \quad (3)$$

where:

z = damping factor ranging between zero and one (for no damping z = 0)

w(n) = the natural angular frequency of oscillation (i.e., the resonance frequency for a single degree of freedom system).

This simple mathematical model is considered sufficient to describe most of the physical systems described in this thesis.

1. Mathematical Expressions for Damping

Damping capacity, a material's ability to absorb vibrational energy and transform it into other forms of energy, can be measured and expressed in a number of related quantities:

a. Logarithmic decrement (δ) for exponential, cyclic free decay:

$$\delta = \ln(A_i/A_{i+1})) = (1/n)\ln(A_o/A_n) = 2\pi z/(1-z^2)^{1/2} \qquad (4)$$

where:

n = number of cycles between A_o and A_n.

b. Normalized bandwidth: Damping measured using the half power point method for evaluating a resonance peak in the system's frequency response to excitation:

$$\text{Normalized Bandwidth} = (\omega_2-\omega_1)/\omega(n) \qquad (5)$$

where:

ω_1, ω_2 = those frequencies framing $\omega(n)$ at which the stored energy is half its maximum value (see Figure (1)). The amplitude at ω_1 and ω_2 is 0.707 times the maximum value.

c. Quality Factor: the quality factor Q measures the sharpness of a resonance peak in the frequency response:

$$Q = \omega(n)/(\omega_2-\omega_1) = 1/2z \tag{6}$$

d. Internal Friction: the inverse of the quality factor, also called the loss factor:

$$\eta = 1/Q = (\omega_2-\omega_1)/\omega(n) = 2z \tag{7}$$

e. Specific Damping Capacity: (SDC) represents the energy dissipated per cycle for an oscillating system in free decay:

$$SDC = (A_{i+1}^2 - A_i^2)/A_i^2 \tag{8}$$

where:

A_{i+1}, A_i = amplitudes at the end and beginning of a cycle.

If $(A_{i+1} - A_i)$ is small, the SDC can be approximated as:

$$SDC = 2(A_{i+1} - A_i)/A_i \tag{9}$$

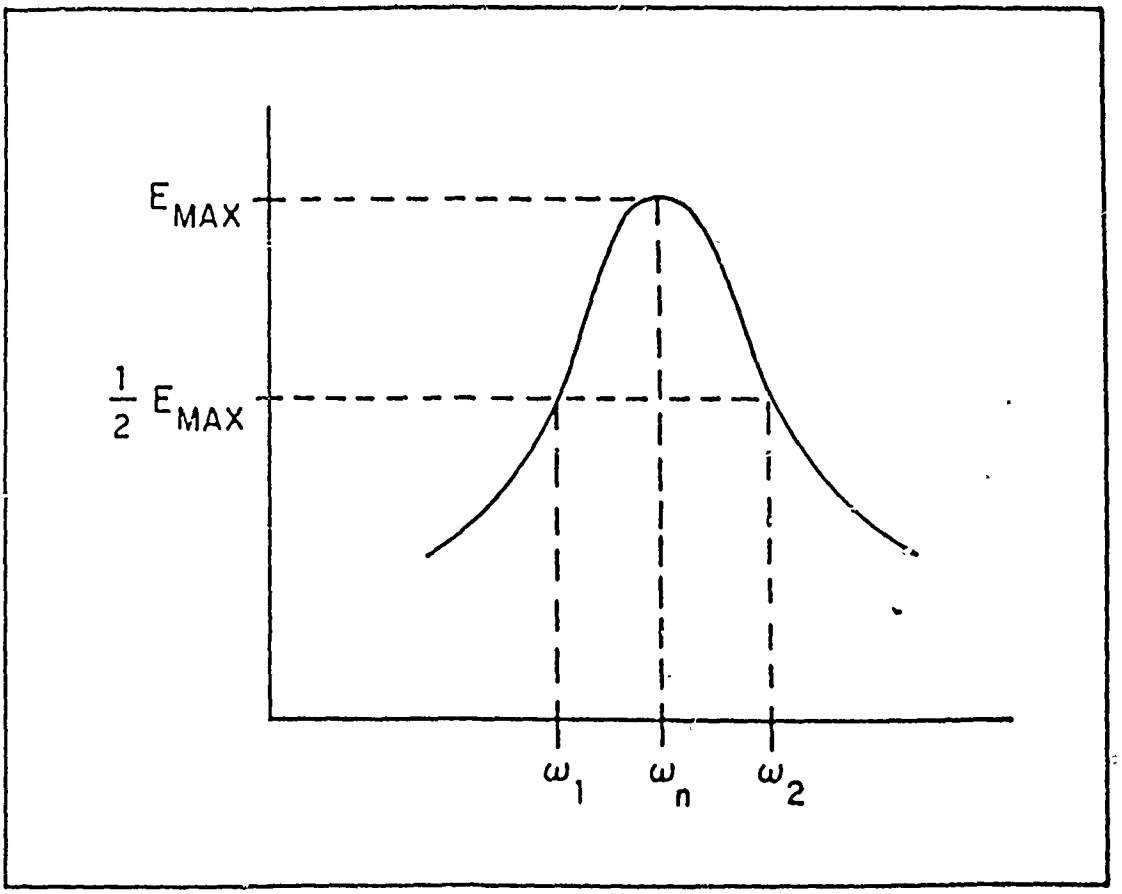

Figure 1. Normalized Bandwidth Used in the Half-Power Point Method of Measuring Damping

SDC, expressed as a percentage, is related to the other expressions for damping as follows:

$$\begin{aligned} SDC(\%) &= 200\pi/Q = 200\pi((\omega_2-\omega_1)/\omega(n)) \\ &= 200\pi\eta = 400\pi\delta \end{aligned} \tag{10}$$

f. Phase Angle: The angle by which a system response lags behind the input excitation:

$$\tan(\phi) = (1/\pi)\ln(A_i/A_{i+1}) = \delta/\pi = 1/Q = \eta = 2z \tag{11}$$

2. Damping Measurement Techniques

A variety of techniques have been developed for measuring the damping capacity of materials and structures. An inverted torsion pendulum apparatus has been frequently used [Refs. 4,5,6] to measure the log decrement of a material undergoing free vibration (i.e., free decay). The single cantilever beam resonance dwell apparatus developed by Bolt, Beranek and Newman, Inc. [Ref. 7] is a popular method for measuring a material's damping characteristics under conditions of continuous forced vibration. Previous research at NPS on high-damping materials, including the Fe-Cr alloys, have used a modified version of this technique [Refs. 8,9,10,11]. A brief description of this technique follows.

An electromagnetic shaker drives the clamped end of a cantilever beam specimen with a continuous forced excitation. Accelerometers mounted at the root and tip of the beam measure the response of the beam to this excitation. A spectrum analyzer processes the signals from the input (root) and output (tip) accelerometers, producing the frequency response of the beam. The half-power point method is used to measure the damping capacity from the resonance peaks which appear in the frequency response. A strain gage mounted at the beam root measures the strain amplitude experienced by the beam at the first modal (resonant) peak. The free vibrational decay of a cantilever beam can also be used to obtain the log decrement of a material [Ref. 12].

The generation and analysis of hysteresis curves to obtain the damping capacity of a material will be described later.

3. Fe-Cr-Based Damping Alloys

Ternary Fe-Cr-Mo and Fe-Cr-Al high damping alloys have been developed independently by Japanese and West German companies. This study considered two Fe-Cr-based alloys similar to the German (Vacuumschmelze, GMBH, Hanau) Vacrosil-010 alloys. Reference should be made to Escue [Ref. 13] and Ahktar [Ref. 14] for information regarding the corrosion characteristics of these alloys in seawater. The chemical composition of these alloys has been analyzed by

two independent analysis laboratories, and is essentially as follows (numbers listed are weight percents):

TABLE 1

CHEMICAL COMPOSITION OF THE ALLOYS STUDIED [REF. 15]

Element	Fe-Cr-Mo	Fe-Cr-Al
Iron	84.7	85.0
Chromium	11.7	11.5
Molybdenum	2.92	-
Aluminum	-	2.95
Carbon	0.007	0.007

Traces (less than 0.002%) of oxygen, nitrogen, sulphur, nickel calcium and about a dozen other elements were also found in the alloys. Table 2 lists some representative engineering properties for these alloys:

TABLE 2

MECHANICAL AND ELECTRICAL PROPERTIES OF THE ALLOYS STUDIED [REF. 16]

Ultimate Tensile Strength	65,264 psi
Yield Strength	46,410 psi
Density	0.2422 lb/in (7.47 g/cm)
Young's Modulus	24.38×10^6 psi
Electrical Conductivity	0.96×10^6 mho/m
Relative Permeability	300

The Fe-Cr-Al and Fe-Cr-Mo alloys evaluated here are of the class of ferritic stainless steels. Ferritic stainless steels have been less widely used in engineering applications than austenitic and martensitic stainless steels due to their relatively poor weldability, susceptibility to embrittlement and notch sensitivity. However, they do possess good corrosion properties, and associated with their ferromagnetism, excellent damping properties.

At room temperature, ferritic stainless steels exist as an alpha phase solid solution with a body-centered cubic (bcc) structure. Ferritic stainless steel alloys usually contain very little dissolved carbon and it usually appears in the microstructure in the form of very fine chromium carbide precipitates. Carbon makes up less than 0.01% of the alloy compositions in the present research. For a discussion of the Fe-Cr phase diagram as it pertains to high damping ferritic stainless steel alloys, see O'Toole [Ref. 8].

4. Damping Properties of Fe-Cr Alloys

The high damping capacity of the Fe-Cr alloys studied in this research is generally accepted to be a magnetomechanical hysteresis mechanism, which will be discussed later. This magnetomechanical phenomenon, and the subsequent damping capacity of the material, is influenced by the following physical parameters.

a. Cold Work [Ref. 17]

Damping capacity is strongly deteriorated by cold work. A reduction of more than five percent completely destroys the damping effect; however, it can be restored by a succeeding heat treatment.

b. Magnetic Field [Refs. 4,8,12,17]

Damping decreases sharply in the presence of a magnetic field. At a certain field level the magnetic domains, and damping, will disappear entirely. Therefore, these alloys should not be used in applications where they will be subjected to magnetic fields exceeding 5000 A/m. Experimental studies of the damping response of these alloys in the presence of varying magnetic fields will be covered later.

c. Magnetic (Curie) Transformation Point

When the temperature of a ferromagnetic material is increased, the added energy reduces the magnetic permeability (magnetization) and permits magnetic domains to become randomly oriented. Above the magnetic transition temperature or Curie temperature, the material becomes paramagnetic (i.e., non-magnetic) and loses all magnetic-related damping properties. The Curie temperature is approximately 725 C for the Fe-Cr-Mo alloy, and is above 700 C for most ferromagnetic alloys.

d. Heat Treatment [Refs. 5,8,9,17]

Annealing these alloys at temperatures in the 900 C to 1200 C range improves the damping capacity over that of a non-treated alloy. The means of cooling used following solution treatment also has an effect on the resulting damping capacity of the material.

e. Stress and Strain [Refs. 4,8,12,17]

Numerous experimental studies have evaluated the strain-dependence of damping capacity in high damping alloys. What follows is a brief summary of some of the most significant of those studies, including previous work at the Naval Postgraduate School. In all of these studies, the general behavior these materials followed was an initial damping capacity increase with increased strain, passing through a maximum damping at a certain critical strain amplitude, and then decreasing.

Kawabe, et al. [Ref. 4] investigated the strain dependence of damping in an Fe-Cr-Al alloy (SILENTALLOY, developed by the Toshiba Corporation). Using the inverted torsion pendulum technique, damping was measured over a strain range of 0-300 microstrain. Maximum damping was achieved at a strain amplitude of about 100 microstrain. Damping measurements were done in the presence of various magnetic field intensities: 0, 3020, 4540, and 15,100 Amperes per meter, respectively. Damping decreased with

increased magnetic field intensity for all strain amplitudes.

Suzuki, et al. [Ref. 12] tested the damping capacity of sintered Fe-Cr-Mo alloys by measuring the log decrement of freely decaying oscillations of various cantilever beam specimens. Experimental results were presented in figures plotting δ vs. beam amplitude, alloy % chromium, sintering temperature and relative density. Additionally, the effect of an external magnetic field on log decrement values was measured through the use of solenoids which either demagnetized the specimen or magnetized it up to 1591 A/m. Damping initially decreased rapidly with increasing magnetic field, reached a minimum at about 4000 A/m (at 50 to 60 percent of the original damping capacity), then increased slightly, levelling out at the maximum field values measured. Damping capacity increased with increased deflection amplitude, passed through a maximum value, then dropped off. A strong damping dependence on porosity, percent chromium and sintering temperature were also noted in these sintered alloys.

Schneider, et al. [Ref. 17] studied the damping properties of a number of Fe-Cr alloys. SDC vs. stress amplitude curves were obtained using the log decrement technique for the Fe-Cr-Al version of Vacrosil-010, for one hour anneals at 1000 and 1100 C. A maximum SDC of 40 percent was obtained with the 1000 C annealed sample.

Damping measurements were also conducted in a magnetic field; it was shown that damping in Vacrosil-010 increases slightly with increased field intensity up to 2000 A/m, then drops off sharply once the field is large enough that it fixes the magnetic domain walls within the specimen.

Masumoto, et al. [Ref. 5] did an extensive study of the heat treatment and strain dependence of damping in Fe-Cr-Mo alloys. A number of different alloys were studied, with molybdenum mass percentage ranging from four to 10 percent and chromium mass percentage ranging from 10 to 20 percent. One hour heat treatments were done at 900, 1000, 1100 and 1200 C, with specimens either furnace cooled or water quenched following heat treatment. Damping capacity was measured using the inverted torsion pendulum technique to obtain log decrement. Results were reported by plotting internal friction vs. maximum shear strain amplitude over a range of 0-300 microstrain. Damping capacity was again seen to increase with increased strain, reach a maximum and then decrease in all specimens. For the alloy most closely resembling the mass percentages of Vacrosil-010, an Fe-10 % Cr-4 % alloy, maximum damping was obtained at about 80-120 microstrain for all heat treatments. For furnace-cooled specimens, damping decreased with decreasing annealing temperature, with a large drop between the 1100 C and 1000 C curves; maximum damping was attained using the 1200 C solution treatment. Maximum damping in the water quenched

specimens was obtained at 1000 C, followed in descending order by the 900 C, 1100 C, and 1200 C specimens. Thus a different relationship between damping and annealing temperature was evident for the two different cooling rates after the anneal.

The next few paragraphs summarize the results of previous research at the Naval Postgraduate School on the heat treatment and strain-amplitude dependence of damping in Fe-Cr-Mo and Fe-Cr-Al high damping alloys.

O'Toole [Ref. 8] tested the damping capacity of an Fe-Cr-Mo alloy (similar to the German Vacrosil-010 alloy) using the modified resonant dwell apparatus. Cantilever beams were annealed for one hour at 800, 900, 1000, and 1000 C and either furnace-cooled or water-quenched. He obtained damping values over a strain range of 0-250 microstrain for all specimens. The water-quenched specimens displayed SDC values in the 5-15% range that were strain-independent. Furnace-cooled specimens showed a strong strain-dependence and followed the previously observed trend of increased damping with increased strain until a maximum is reached, then falling off. Table 3 summarizes the results of O'Toole's damping work. O'Toole speculated that annealing relieves residual stresses which would reduce damping in non-annealed specimens. Furthermore, the quick cooling rate attained through water-quenching reintroduces residual stresses in the material, and thus explains the low

TABLE 3

MAXIMUM SDC AND PEAK STRAIN AMPLITUDE FOR FE-CR-MO ANNEALED AT VARIOUS TEMPERATURES AND FURNACE COOLED [REF. 9]

Anneal Temp. (C)	Max SDC (%)	Peak Strain ($\times 10^{-6}$)
800	36.21	155.0
900	49.01	67.1
1000	36.35	126.4
1100	54.72	72.7

damping obtained in those specimens. The drop in SDC for the 1000 C specimen was curious, and O'Toole examined optical micrographs and conducted X-ray diffraction in determining whether a phase change at that temperature contributed to the decreased damping. No evidence of a phase change was found.

Ferguson [Ref. 9] studied the relation between heat treatment, strain amplitude and damping in both the Fe-Cr-Mo and Fe-Cr-Al alloys. Using a different resonant dwell apparatus than O'Toole, he obtained damping data over a strain range of 0-50 microstrain for cantilever beam specimens annealed at 950, 1000, 1050 and 1100 C. Within this strain range damping values increased and reached a maximum at about 10 microstrain; however, only for the Fe-Cr-Mo alloy annealed at 1000 C were strain amplitudes obtained that were high enough to display the post-maximum damping decrease found in the other studies. He obtained

maximum damping values in the SDC range of 45-60% for all of his specimens, with the 1050 C annealed specimens yielding the highest damping values for both alloys.

Ferguson also conducted tensile tests on these alloys and discovered low strain nonlinearities in the stress-strain diagrams. He attributed these nonlinearities to the hysteresis phenomenon inherent in these materials. Ferguson also searched for evidence of a phase change within the range of the annealing temperatures, using dilatometry, with negative results.

Cronauer [Ref. 10] used the same resonant dwell apparatus as Ferguson in testing the temperature dependence of damping in cantilever beams tested at temperature ranges of 22 C, 36-41 C, 60-69 C, and 92-109 C. No temperature dependence of damping was evident over this range. Cronauer concluded that the damping behavior was insensitive to temperature changes up to 109 C, and probably up to temperatures approaching the Curie temperature. Maximum SDC values of 60-65% were obtained at a peak strain amplitude of five microstrain.

Patch [Ref. 11] developed a computerized data acquisition system for handling damping data obtained with the modified resonant dwell apparatus used by Ferguson and Cronauer. He also attempted to image the ferromagnetic domains via transmission electron microscopy, but due to the

configuration of the particular TEM used, this proved to be impossible.

5. Microstructural Damping Mechanisms in Fe-Cr Alloys

According to de Batist [Ref. 18], damping in ferromagnetic materials occurs primarily as a result of the nonlinear, magnetomechnical hysteresis phenomenon. A secondary possible source of damping is the presence of dislocations in the material. Dislocations in a crystalline material may be expected to move as a material is cyclically stressed, resulting in internal absorption of energy. A third possible source of damping is due to the effect of phase changes in the material; however this does not appear to be relevant in the case of the Fe-Cr-Mo and Fe-Cr-Al alloys studied here.

A brief, straightforward explanation for the basis of magnetomechanical hysteresis in ferromagnetic materials is provided by Cochardt [Ref. 19], and is as follows:

> The energy dissipated during a stress-strain cycle as a result of the magneto-mechanical effect is generally caused by the irreversible magnetostrictive strain. Every ferromagnetic material consists of so-called domains which are more or less randomly oriented in an unmagnetized material. However, on the application of a magnetic field, or a stress, these domains tend to align themselves in the direction of the field, or in the direction of the tension strain. This movement of the domains results in an irreversible change of the dimensions of the material which is called 'magnetostriction.' Accordingly, when a stress strain curve for an unmagnetized ferromagnetic material is recorded, more strain is measured than postulated by Hooke's Law. . . . On relieving the load, the elastic strain reverts to zero, assuming plastic strain is negligible, but the magnetostrictive strains

remains almost constant; in other words, the curve follows a hysteresis loop. The greater the area of the loop, the larger the damping capacity of the material. . . .

Cochardt expresses damping capacity in terms of the logarithmic decrement $d = \Delta w/2w$, where w is the mean elastic energy of the specimen and Δw is the energy dissipated in the specimen per cycle per unit volume. He also presents the concept of a critical stress, at which damping in a ferromagnetic material reaches a maximum. For a cantilever beam, where stress conditions closely correspond to those in vibrating blades, shafts, etc., Cochardt's development concludes that the critical stress is approximately 40 percent of the maximum normal stress.

Cochardt also observed that, due to the magneto-mechanical effect, the areas of magnetic and mechanical hysteresis loops are proportional to each other. Additionally, he noted that certain high damping alloys do not exhibit appreciable damping when tested in a strong magnetic field. Willertz [Ref. 6] observed this as well. He used an inverted torsion pendulum to measure the damping in Fe-12% Cr specimens under applied axial and static torsional stresses. An applied magnetic field of 47,800 Amperes per meter was found to completely suppress magneto-mechanical damping in the sample. Subtracting the damping measured in the presence of the magnetic field from that measured without the magnetic field enabled him to determine the damping solely attributable to the magneto-mechanical

phenomenon. His results proved that magneto-mechanical damping is the dominant mode of damping in ferromagnetic alloys. Work by Kawabe [Ref. 4], Suzuki [Ref. 12] and Schneider [Ref. 17] previously mentioned supported these conclusions and provided additional experimental work on the influence of an external magnetic field on damping in Vacrosil-010 and similar Fe-Cr-based alloys.

6. Analysis of Stress-Strain Hysteresis Loops

Nashif, Jones and Henderson, in their book entitled Vibration Damping [Ref. 20], acknowledge ferromagnetic hysteresis as being the dominant mode of damping for "typical constructional metal alloys and even some high damping alloys." The cusped, nonlinear shape of the hysteresis curve shown in Figure 2 is cited as being a common feature when a nonlinear mechanism is responsible for the observed damping. In the case of so-called linear viscous damping mechanisms, the observed hysteresis loop is elliptical with a straight-line major axis.

Analytical representations of a nonlinear hysteresis loop have been developed, many of which are presented in Reference 20. An example of these is the following:

$$\vec{\sigma} = E\{e \pm \nu/\eta[e(o)-e)^n - 2^{n-1} e(o)]\} \qquad (12)$$

or

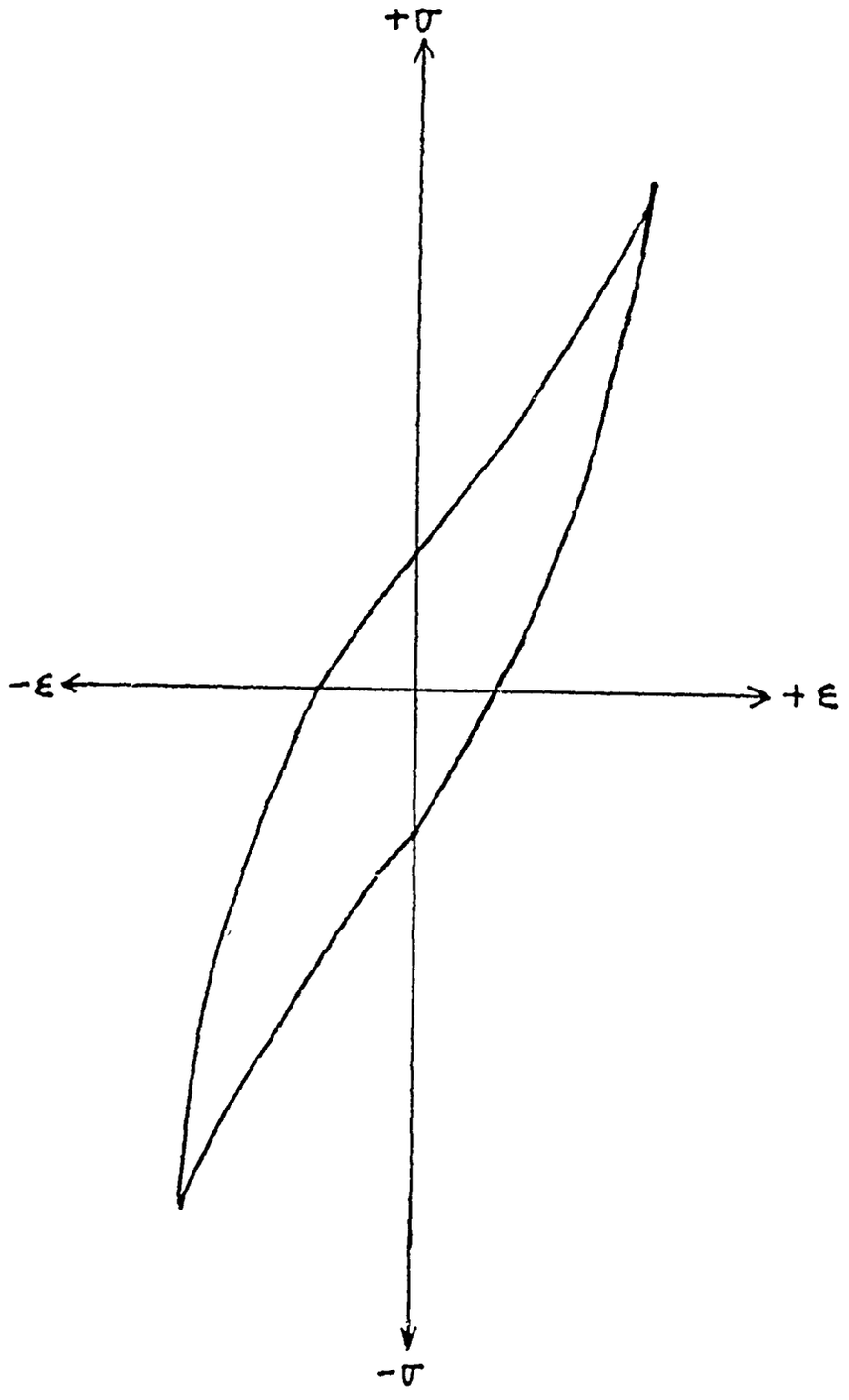

Figure 2. Typical Nonlinear Hysteresis Loop Obtained from the Stress-Strain Response of a Ferro-Magnetic Material

$$\overset{\rightarrow}{\sigma}_{\leftarrow} = E(e)\{e \pm \eta(e)e(o)|1 - (e/e(o))^2|^n\} \qquad (13)$$

where:

$E(e)$ = the strain dependent elastic modulus

$\overset{\rightarrow}{\sigma}$ = stress during the loading part of the cycle

$\overset{\leftarrow}{\sigma}$ = stress during the unloading part of the cycle

e = strain

$e(0)$ = maximum strain

n = an empirical hysteresis parameter

$\eta(e)$ = the strain dependent system loss factor

ν = Poisson's ratio.

In plotting σ vs. e for all instants of a cycle of a sinusoidally oscillating system, a hysteresis loop is obtained. The energy dissipation during a cycle of deformation per unit volume of the specimen material is:

$$\Delta w = \oint \sigma de = \int_0^{2\pi/w} (de/dt)\, dt = \pi\eta E e(o)^2 \qquad (14)$$

The maximum energy stored in the specimen is

$$w = 0.5Ee(o)^2 \qquad (15)$$

Therefore the loss factor can be expressed as

$$\eta = \Delta w/2\pi w \qquad (16)$$

and the specif damping capacity is

$$SDC\ (\%) = 200\,\pi\eta = 100(\Delta w/w) \qquad (17)$$

Nashif, Jones, and Henderson [Ref. 20] give many examples of how hysteresis loops can be analyzed to obtain damping parameters, the strain dependent elastic modulus, etc. The loss factor and modulus are dependent on both frequency and temperature; however, it is stated that and E can be assumed constant over a limited range of frequencies and temperatures.

Ray, Wren and Kinra [Ref. 21] are currently conducting material damping measurements on an Al 6061-Mg-Zr metal matrix composite via direct quantitative analysis of hysteresis loops obtained by the axial loading of tensile specimens in an MTS mechanical testing system. Their approach utilizes the trapezoidal area approximation in measuring the areas on a stress-strain diagram within and underneath a hysteresis loop, the ratio of which represents the specific damping capacity of the specimen (see Figure 3). Sinusoidal oscillation of the loads produced the observed hysteresis loops, in which stress and strain varied in accordance with the following:

$$\sigma = \sigma(o) + \sigma(a) \cos\ wt \qquad (18)$$

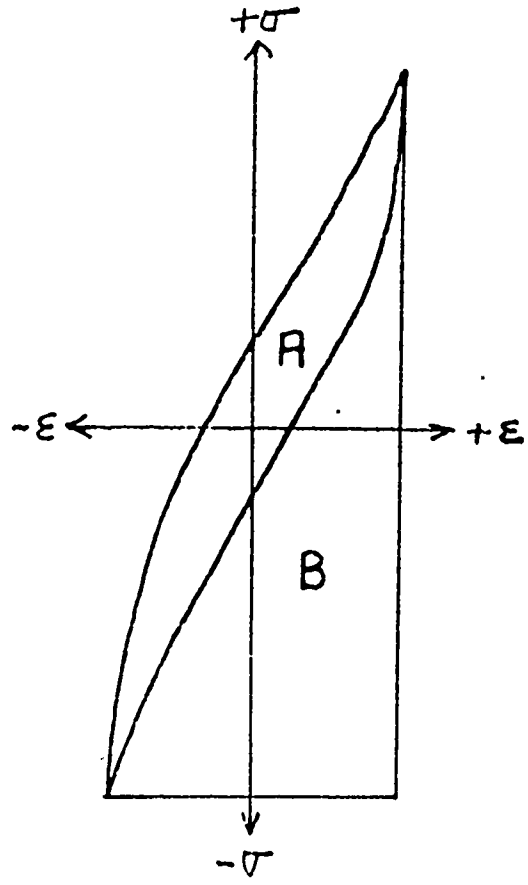

$$SDC = \frac{\Delta W}{W} = \frac{AREA(A)}{AREA(A+B)}$$

Figure 3. Damping Measurement from the Areas in a Stress-Strain Hysteresis Curve

$$e = e(o) + e(a) \cos (wt - \phi) \qquad (19)$$

where:

$\sigma(o), e(0)$ = the mean stress or strain

$\sigma(a), e(a)$ = the alternating stress or strain

σ, e = the instantaneous stress or strain

ϕ = the phase lag between strain and stress, and

w = the angular frequency of oscillation.

Their specimens were tested over a 30-2000 microstrain strain range and a 0.1-10.0 Hz frequency range. This research concentrated on determining how damping varied with the matrix orientation within the specimen. It demonstrated the usefulness of this simple but reasonably accurate method for measuring material damping over strain ranges higher than those previously obtained using the more common log decrement or half power-point methods presented earlier.

C. OBJECTIVES

Previous damping studies at the Naval Postgraduate School have used the resonant dwell apparatus to obtain SDC as a function of cyclic strain amplitude at quite low strains. The objective of the present research was to examine other techniques for measuring the damping response of high damping alloys, to use higher strain amplitudes than achieved previously, and to link together the damping

results obtained for all the ranges of strain amplitude studied.

II. EXPERIMENTAL PROCEDURE AND DESCRIPTION OF DATA ANALYSIS

Button-end tensile specimens were prepared in accordance with the dimensions and specifications indicated in Figure 4. Some of these specimens were machined from an ingot of the Fe-Cr-Mo alloy; the others were machined from an ingot of the Fe-Cr-Al alloy. The specimens were annealed for one hour in a tube furnace under flowing argon gas (to minimize oxidation of the specimen surfaces during heat treatment) at temperatures of 900 C and 1100 C. Specimens were allowed to furnace cool to room temperature.

An MTS (Mechanical Test System) Machine was used to subject the specimens to sinusoidally alternating compressive and tensile axial loads. Five different load levels were used, corresponding to the maximum and minimum stress and strain levels listed in Table 4. The highest stress level corresponds to about 38 percent of the approximate yield stress for these alloys.

Axial displacement of the specimens in response to the alternating loads was measured using an MTS longitudinal extensometer with a 0.5 inch gage length. Load-displacement data, in the form of a hysteresis loop, was obtained graphically using a plotting device. Additionally, numerical load-displacement data were obtained using the F_Collect data collection program developed here at NPS for

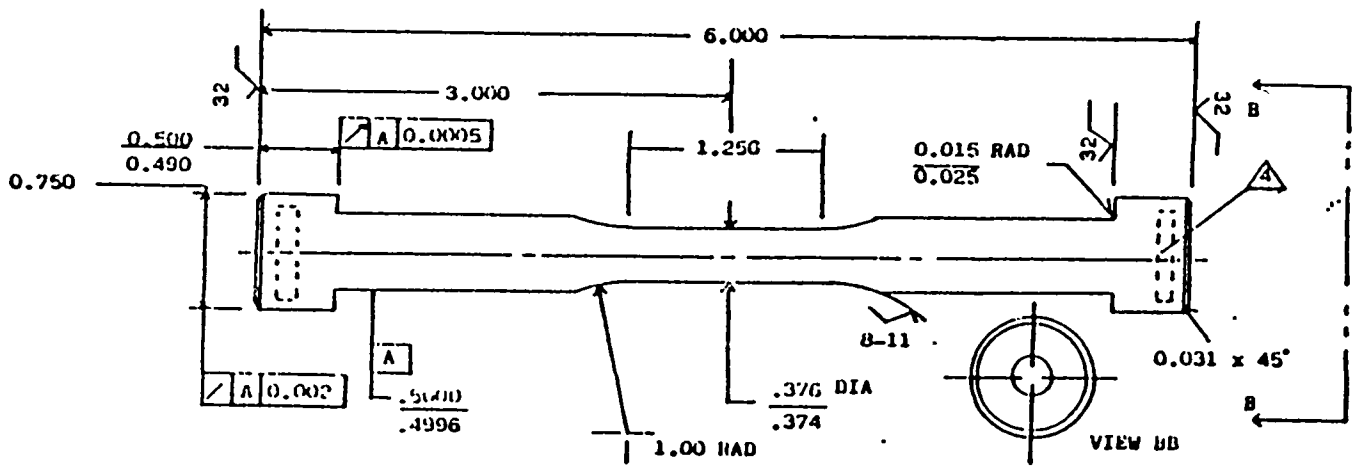

Figure 4. Geometry and Dimensions of the Button-Ended Tensile Test Specimen

TABLE 4

MAXIMUM AND MINIMUM AXIAL LOAD, STRESS AND STRAIN LEVELS USED FOR THE GENERATION OF HYSTERESIS LOOPS

Max Load (lbs)	Max Stress (psi)	Max Strain (μs)
400	3636	160
800	7273	300
1200	10909	525
1600	14545	685
2000	18182	850

data collection on the MTS testing machine. The program is run on a Hewlett-Packard 9826 computer; data collection is controlled by a Hewlett-Packard 3497A Data Acquisition/ Control Unit and a Hewlett-Packard 3437A system voltmeter. Hysteresis loops were generated at each loading level for each specimen over a frequency range of zero to ten hertz. The F_Collect data collection program is listed in Appendix A.

The strain energy dissipated per cycle (Δw) and total strain energy (w) was obtained by measuring the areas within and underneath the hysteresis loops using the trapezoidal area approximation. The ratio of these two areas ($\Delta w/w$) represents the specific damping capacity of the specimen under those loading conditions at that frequency. Since a ratio is calculated the load-displacement hysteresis loops can be used directly in determining damping, as all units

cancel and the SDC ratio is dimensionless. Maximum strain values per cycle were obtained using the maximum displacement per cycle in each loop and the strain relationship:

$$e(\text{true}) = \ln[(l_o + \Delta l)/l_o] = \Delta l/l_o = e(\text{eng}) \qquad (20)$$

where:

Δl = instantaneous displacement at maximum loading

l_o = gage length = 0.5 inches.

At low strain levels the true strain and engineering strain are approximately equivalent. The maximum strains varied slightly between loops obtained at different frequencies at a given loading; the maximum strain values presented in Table 4 here are averages for all the hysteresis loops generated at that loading.

III. RESULTS AND DISCUSSION

A. QUALITATIVE ANALYSIS OF HYSTERESIS LOOPS

A set of typical hysteresis loops obtained during cyclic axial loading of an Fe-Cr-Al tensile specimen over a 10 hertz frequency range is shown in Figures 5 and 6. This particular specimen had been annealed for one hour at 1100 C and furnace-cooled; the maximum stress-strain levels were 3620 psi and 160 microstrain, respectively. This figure is representative of the hysteresis loops generated for various specimens at various loading levels. The hysteresis loop starts out very narrow at low frequencies, representing very little energy dissipated per cycle; that is, low damping. With increased frequency the loop opens up and becomes wider, enclosing a greater area and thus indicating increased damping. At a certain frequency a maximum area is obtained, and maximum damping is achieved. As frequency is increased still further, the loop "collapses" and the area enclosed by the loop is reduced, indicating a decrease in damping.

As well as the enclosed area, the shape of the hysteresis loop changes with frequency. At the lowest frequencies examined here (1 to 4 Hz) the loop has the cusped, nonlinear shape expected with a material in which a nonlinear damping mechanism is dominant. At slightly higher

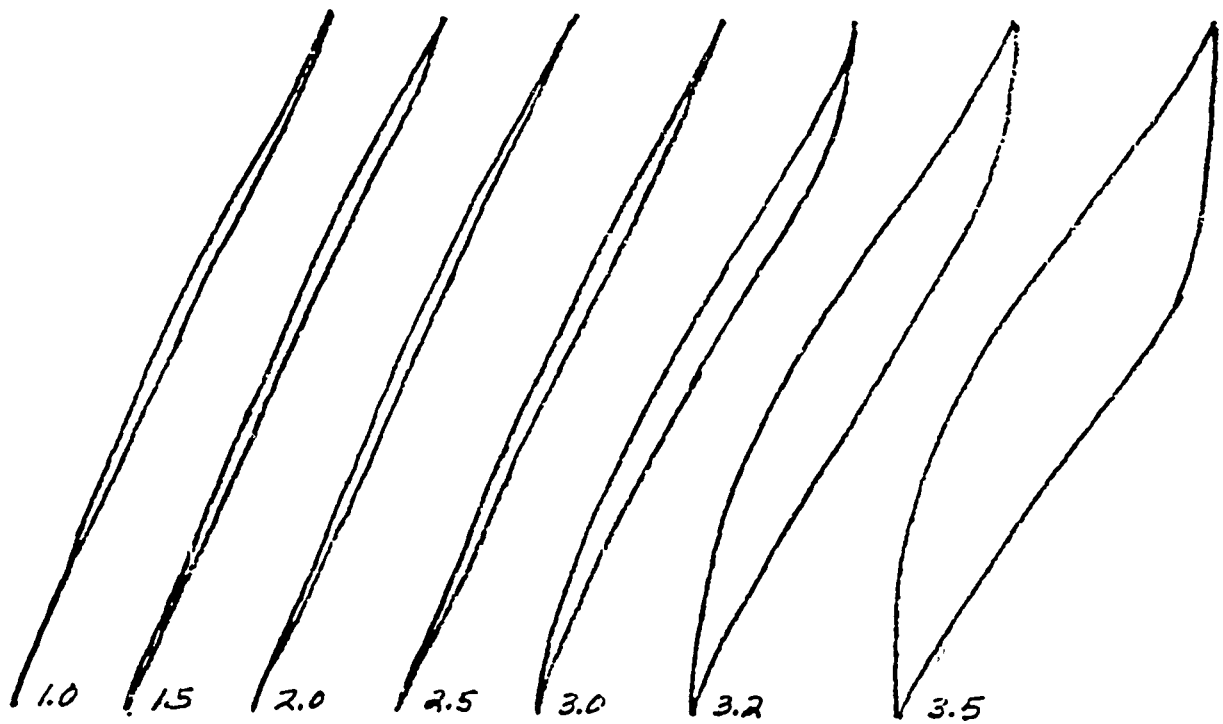

Figure 5. Load vs. Displacement Hysteresis Loops from a Fe-Cr-Al Tensile Specimen Annealed for One Hour at 1100 C Subjected to Cyclic Axial Loading of ±400 lbs, 1.0-3.5 Hz

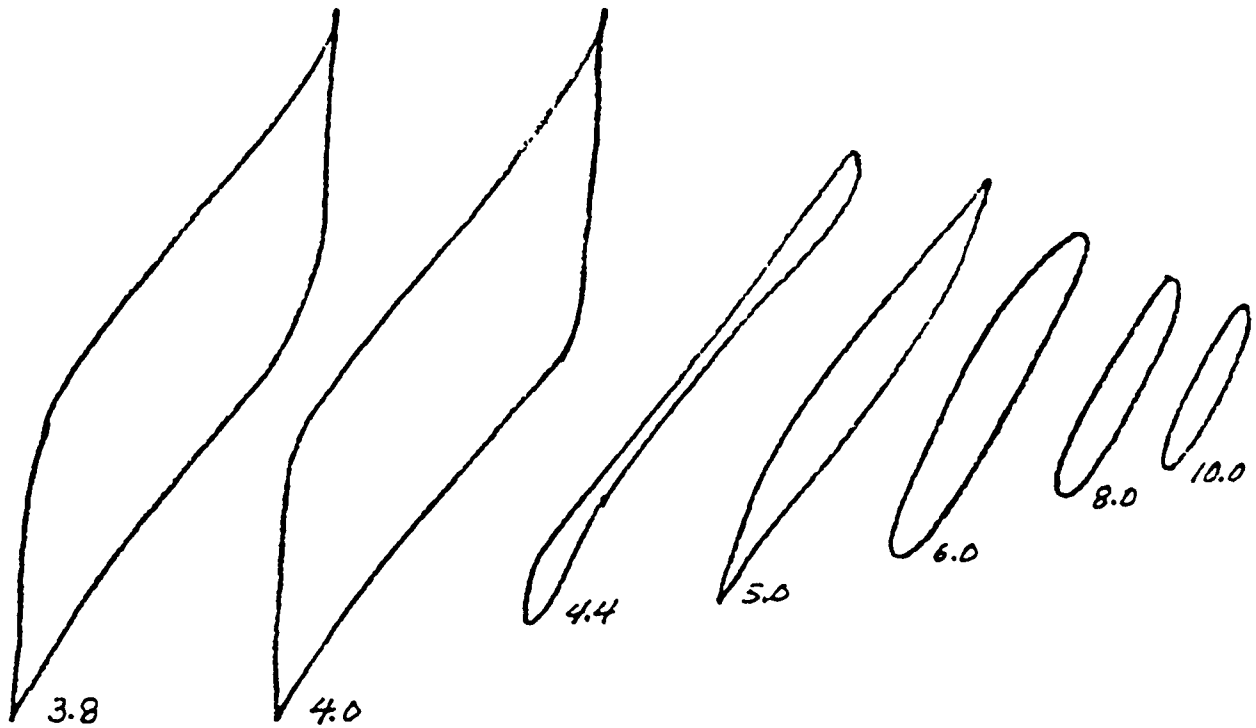

Figure 6. Load vs. Displacement Hysteresis Loops from a Fe-Cr-Al Tensile Specimen Annealed for One Hour at 1100 C Subjected to Cyclic Axial Loading of ± 400 lbs, 3.8-10.0 Hz

frequency (5 to 10 Hz) the loops become elliptical with a straight-line major axis. The loops in Figures 5 and 6 also appear to be getting smaller, but this is actually due to the plotting device being unable to extend through the compressive and tensile loading maximums at high frequencies, resulting in a rounding off of the corners of these loops. The numerical data obtained with the F_Collect data acquisition program enabled confirmation that the high frequency hysteresis loops were elliptical and were passing through the maximum loads and displacements, as shown for example in Figure 7, which is a representative example of a high frequency hysteresis loop plotted from numerically acquired data.

As previously mentioned, the trapezoidal area approximation was used in the calculation of the relevant areas used to determine damping. This method, although tedious, proved to be a fairly accurate method provided a reasonable number of intervals are used. Use of the more accurate Simpson's Rule area approximation did not change the calculated damping values greatly.

A more accurate method for calculating the areas enclosed by the hysteresis loop would consist of a computer program which would use the numerical data obtained by the F Collect system to calculate the area exactly. Such a program was developed; however, problems with the data acquisition system precluded its utilization. The main

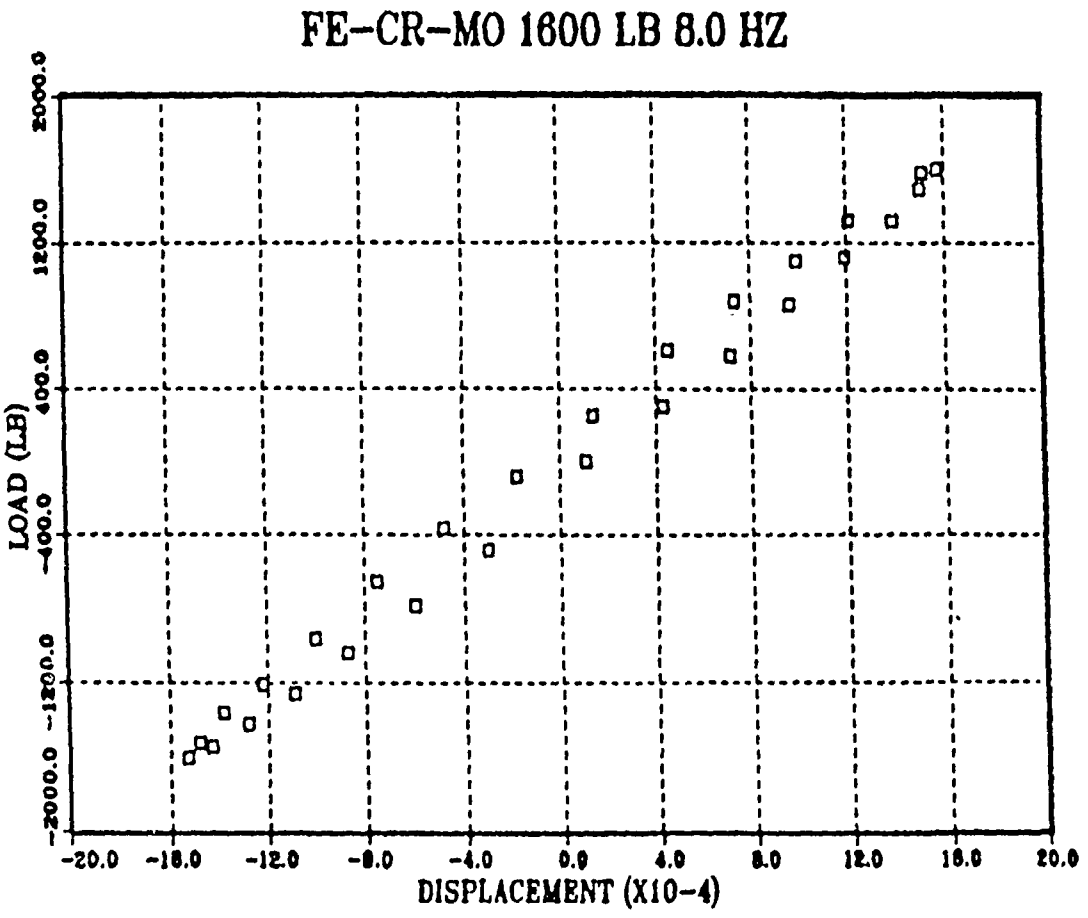

Figure 7. Load vs. Displacement Hysteresis Loop from a Fe-Cr-Mo Tensile Specimen Annealed for One Hour at 1100 C Subjected to Cyclic Axial Loading of ± 1600 lbs, 8.0 Hz

problem with the data acquisition system was that it typically "dropped out" of the loop after one quarter or one half of a cycle, and generated "garbage" data pairs thereafter. The data acquisition was not designed to collect load-displacement data pairs at the speed needed to capture a hysteresis loop. As a result, only a few data runs provided a complete set of data over a full load-displacement cycle. Appendix B contains the area-calculating program used in conjunction with F_Collect.

Since the numerical data were incomplete for all but a few instances, and since the high frequency hysteresis loops were not accurately plotted by the plotting device, the areas enclosed by these loops had to be estimated. This was done by assuming that each high-frequency loop was elliptical in shape and passed through the load and displacement maximums as shown in Figure 7. In cases where numerical data were complete and the actual areas could be calculated, the estimated areas agreed to within 10 percent.

Figures 8, 9, 10, and 11 are plots of specific damping capacity (SDC) vs. frequency for each of the four specimens tested. For each specimen the damping is seen to be greatly dependent on frequency, increasing rapidly with frequency until a maximum is reached and then dropping off with increased frequency. The frequency at which the maximum SDC is obtained decreases with increased loading; i.e., the damping vs. frequency curves move to the left when the

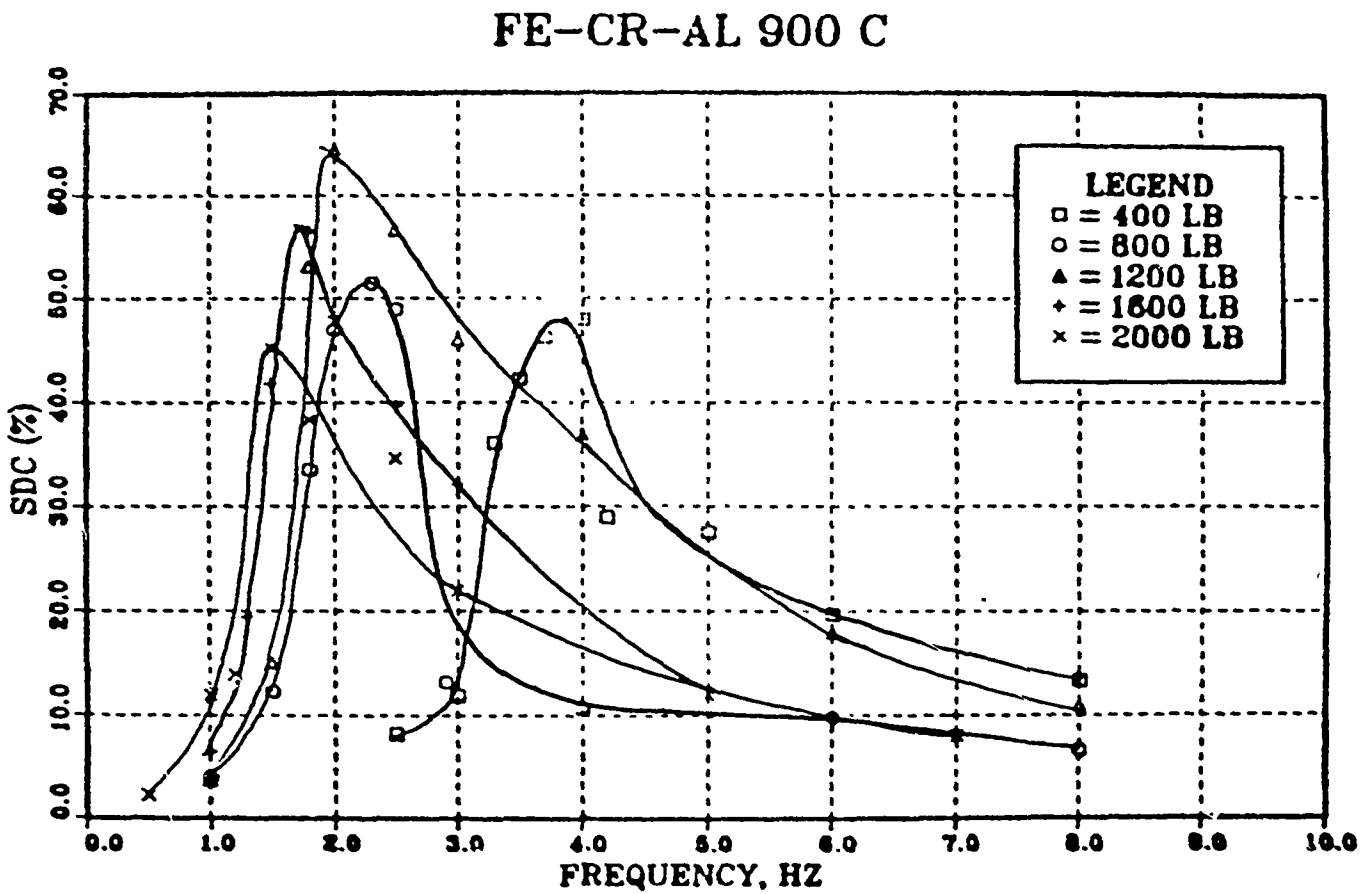

Figure 8. Specific Damping Capacity vs. Frequency from a Fe-Cr-Al Tensile Specimen Annealed for One Hour at 900 C Subjected to Cyclic Axial Loadings of ± 400, 800, 1200, 1600 and 2000 lbs

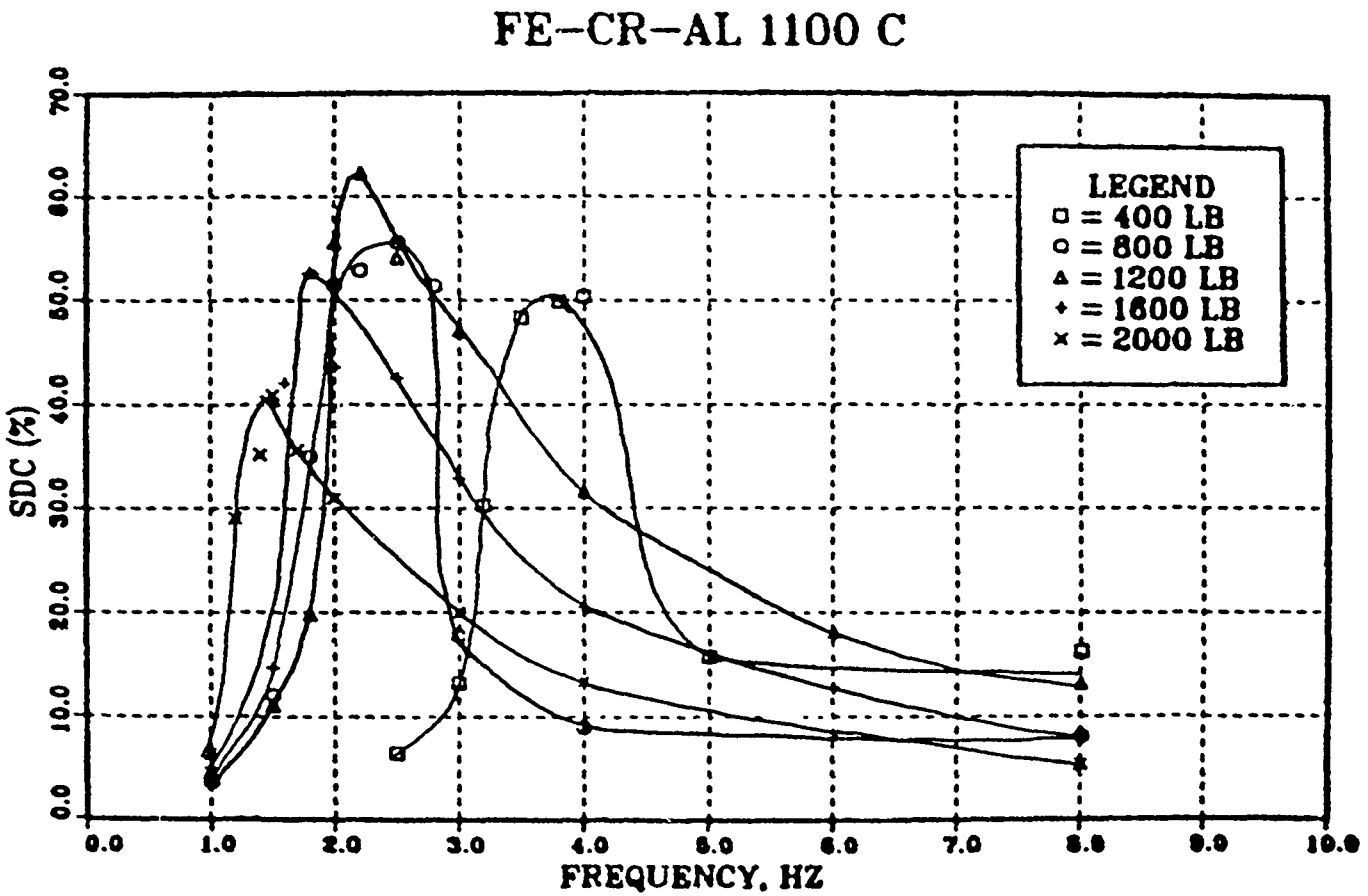

Figure 9. Specific Damping Capacity vs. Frequency from a Fe-Cr-Al Tensile Specimen Annealed for One Hour at 1100 C Subjected to Cyclic Axial Loadings of ± 400, 800, 1200, 1600 and 2000 lbs

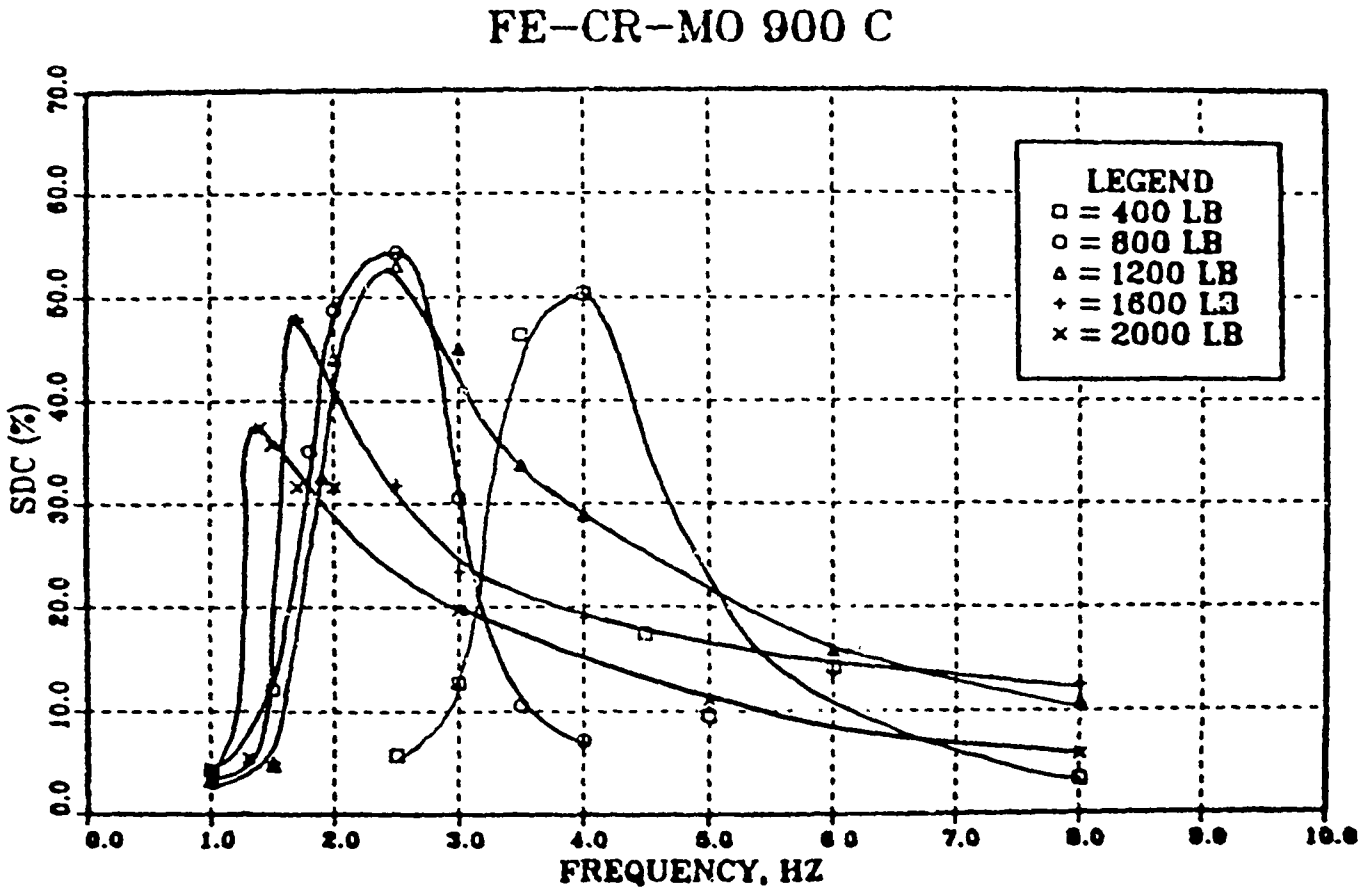

Figure 10. Specific Damping Capacity vs. Frequency from a Fe-Cr-Mo Tensile Specimen Annealed for One Hour at 900 C Subjected to Cyclic Axial Loadings of ± 400, 800, 1200, 1600 and 2000 lbs

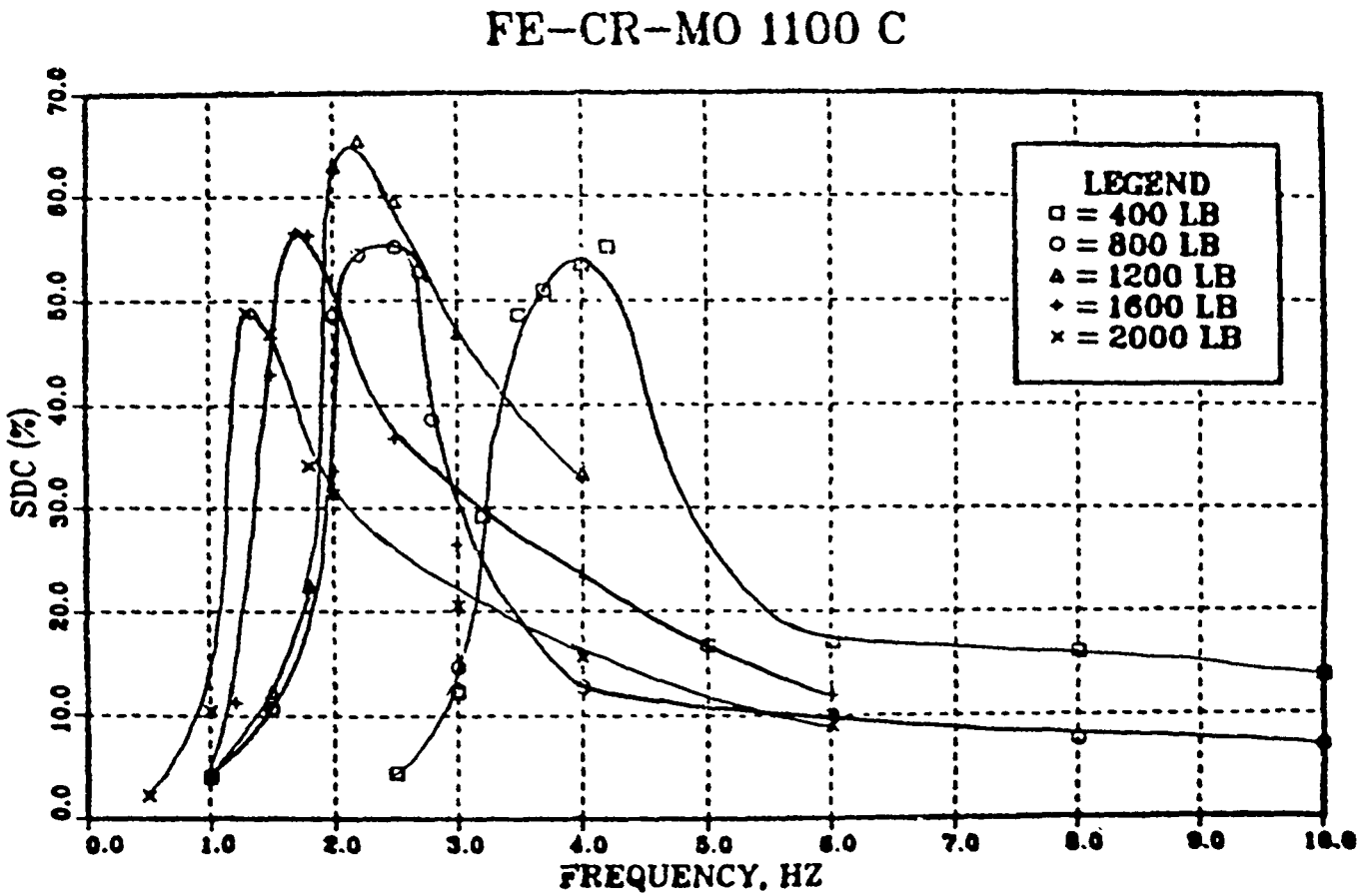

Figure 11. Specific Damping Capacity vs. Frequency from a Fe-Cr-Mo Tensile Specimen Annealed for One Hour at 1100 C Subjected to Cyclic Axial Loadings of ± 400, 800, 1200, 1600 and 2000 lbs

loading level is increased. Tabulated data on which Figures 8 through 11 are based are presented in Appendix C.

Maximum SDC was obtained at the 1200 lb load level for all specimens. This corresponds to a maximum stress and strain level of 10,909 psi and 525 microstrain, respectively. Figure 12 is a plot of maximum SDC vs. loading, stress and strain level. This plot has the same shape as the damping vs. strain relationships found in all the previously cited experimental results measuring damping in high damping Fe-Cr-based alloys. Damping is seen to increase with increased strain amplitude, reach a maximum and then decrease.

Table 5 lists the maximum damping capacities obtained for each specimen at the 1200 lb load level.

TABLE 5

MAXIMUM SDC OBTAINED BY THE FOUR SPECIMENS

Alloy	Annealing Temp.	Maximum SDC
Fe-Cr-Al	900 C	64.36%
Fe-Cr-Al	1100 C	62.24%
Fe-Cr-Mo	900 C	54.22%
Fe-Cr-Mo	1100 C	65.32%

Due to the small number of samples and heat treatments examined, no conclusions regarding heat treatment effects on damping can be made. However, the dependence of damping on

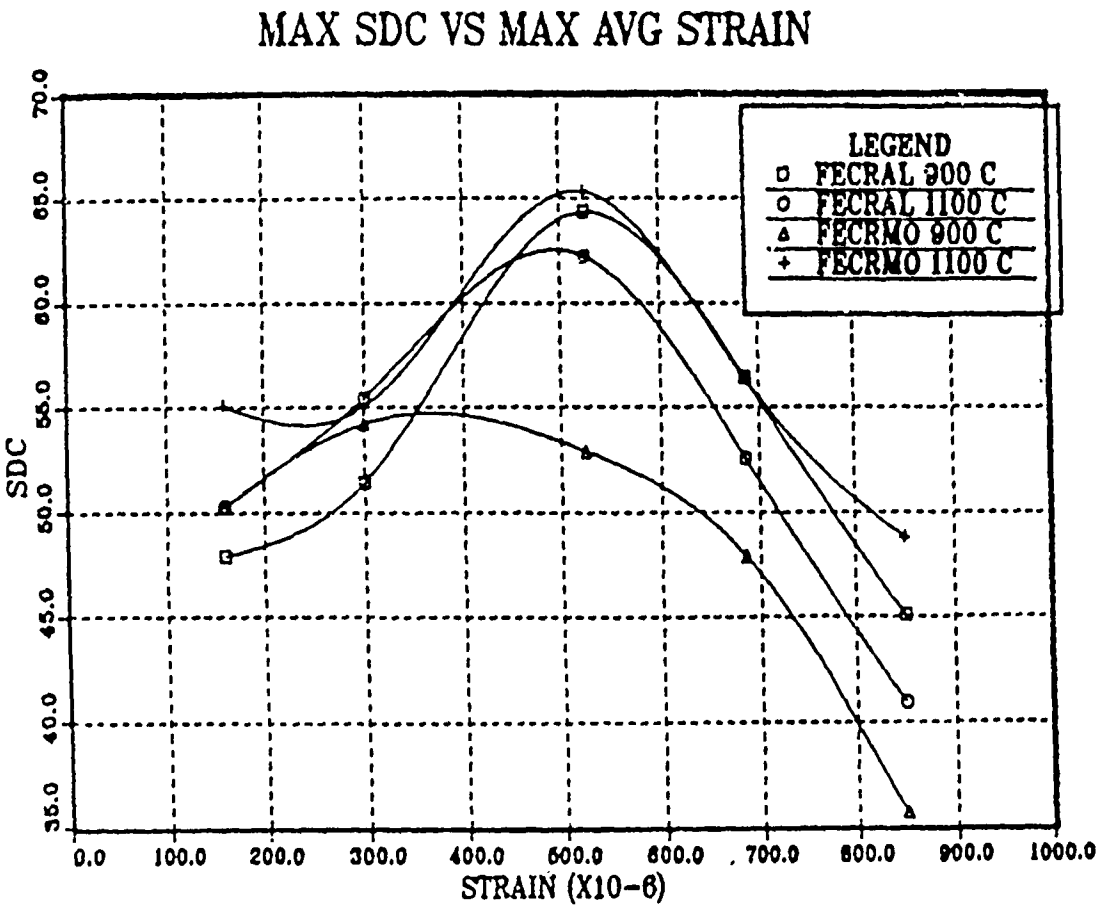

Figure 12. Maximum Specific Damping Capacity vs. the Average Maximum Longitudinal Strain

heat treatment has been firmly established by previous research. The maximum SDC damping values obtained are all in the 50-65% range, as were those obtained using the half power point method for cantilever beams randomly vibrated at much lower strain amplitudes. This similar damping response within completely different strain ranges (160-850 μs here, compared with 0-10 μs and 0-300 μs in previously mentioned findings) makes it difficult to link the independent results in order to make any general observations.

The strong frequency dependence of the damping response of these materials as measured using the hysteresis loop analysis was unexpected for such a small frequency range. Concrete physical explanations for this result cannot be readily made, although it is suspected the frequency dependence must manifest itself on a sub-microstructural level, influencing the interactions of atoms and the movement of the magnetic domains within the material.

IV. CONCLUSIONS AND RECOMMENDATIONS

Analysis of the areas defined by a load displacement hysteresis loop is a simple and reasonably accurate method for measuring the damping response of materials at higher strain amplitudes than those achievable via the resonant dwell or inverted torsion pendulum methods. Further research should attempt to explain the frequency dependence of damping measured this way and also explore possible reasons why the damping response of Fe-Cr based alloys is similar in different regions of strain.

The damping peak in the presented SDC vs. frequency data plots is very sharp, and additional hysteresis measurements should be made in the vicinity of the maximum to define the peak damping more accurately. Additional hysteresis measurements at higher and lower loading levels than those done here could be done to extend the range of damping vs. strain data obtained using this method, thus defining the SDC vs. strain dependence more completely.

Finally, development of a data acquisition system able to collect reliable numerical hysteresis data from the MTS testing machine would allow exact and direct calculation of damping capacity from the hysteresis loops.

APPENDIX A

F_COLLECT DATA ACQUISITION PROGRAM

```
10  !This program is F_COLLECT, a modified version of
20  !a program written by Ken Ellison for data
30  !collection on the MTS testing machine
40  !with data collection controlled by the
50  !HP 9826 computer, HP 3497A Data acquisition/
60  !control unit, and the HP 3437A system
70  !voltmeter  (29 Sep 1987)
80  !
90  !The time for sampling in this program is
100 !governed by the total number of samples
110 !based on 2 bytes/point and the delay
120 !  The sampling is uniform so by sampling 2
130 !channels the time between data POINTS on
140 !same channel is 2X the delay time and the
150 !total time is the number of points times
160 !the delay time
170 ! (500 points)x(.002 sec delay)=1.0 sec
180 !  500 data points= 250 data pairs
190 !*****************************************
191 ON ERROR GOTO Errcheck
200 PRINT "PROGRAM NOW LOADING"
210 PRINT
220 PRINT "In the present form of the program the"
230  PRINT "TOTAL TEST TIME IS ABOUT 1.0 SECONDS"
240  PRINT
250 COM /Hp3054/ Scn,Dvm,Svm,Prt,Error,Err$[6],Ercnt$[15]
260 DIM Y(1:250),X(1:250),In$[1000],Out(1000),Name$[50]
270 BEEP
280 INPUT "What is your load range (1-4):",Lr
290 If Lr=1 THEN Lf=2    !2 kips/volt
300 IF Lr=3 THEN Lf=1    !1 kip/volt
310 If Lr=3 THEN Lf=.4   !.4 kps/volt
320 IF Lr=4 THEN Lf=.2   !.3 kips/volt
330 BEEP
340 INPUT "What is your strain range (1-4):",Sr
350 IF SR=1 THEN Sf=.01     !Longitudinal extensometer
360 IF Sr=2 THEN Sf=.005
370 IF Sr=3 THEN Sf=.002
380 IF Sr=4 THEN Sf=.001
390 PRINT "Press 'continue' to initialize the STRAIN & LOAD"
400 PRINT "MTC IN HIGH PRESSURE!!!"
410 BEEP 300,.5
420 BEEP 450,.75
430 PAUSE
```

```
440 CLEAR 709   !CLEARS THE DVM
450 OUTPUT 724;"DCLAR"    !CLEARS THE DA/CU
460 OUTPUT 724;"T1FN4SD.2S"
470 OUTPUT 709;"AC1AF4AL5AE2"
480 ENTER 724;T,U,V
490 J=0
500 PRINTER IS 706
510!PRINT T,U,V
520 Disv=V
530 Dis0=Disv*SF    !Initial displacement
540 Lodv=U
550 Lod0=Lodv*Lf    !Initial load
560 PRINTER IS 706
570 PRINT
580 PRINT "Initial displacement is";Dis0;"in or";Disv;"volts
590 PRINT "Initial load is ";Lod0;"kips or ";Lodv;"volts
600 PRINT
610 PRINTER IS 1
620 BEEP 300,.5
630 BEEP 450,.75
640 PRINT
650 PRINT "Press 'continue' when you are READY TO TEST."
660 PRINT "PRESS 'CONTINUE' TO START DATA ACQUISITION"
670 PRINT "THEN PRESS 'HOLD' ON THE MTS TO START THE TEST"
680 PRINT
730 CLEAR 709
740 OUTPUT 709;"AC2AC1VNA"
750 OUTPUT 724;"DCLF3D.010S"
760 PAUSE
770 !
780 ! Data acquisition portion
790 !
800 OUTPUT 724;"T1N500SD.002S"
810 OUTPUT 709;"AF4AL5AE2"
820 ENTER 724;In$
830 WAIT 1
840 PRINT
920 PRINT "Data acquisition is complete"
930 PRINT "Data conversion will take about 2 minutes
940 !Input from the DVM the array of data strings
950 J=0
960 !
970 ! String conversion of the data to voltages
980 !
990 !*************Change step size below ******
1000 FOR I=1 TO 1000 STEP 2     !2 bytes/data point
1010 J=J+1
1020 B1=NUM(In$[I])
1030 B2=NUM(In$[I+1])
1040 OUT(J)=(2*BIT(B1,5)-1)*10^(BIT(B1,6)*(BIT(B1,7)-2))
1050 Out(J)=Out(J)*BIT(B1,4)+BINAND(B1,15)+.1*SHIFT(B2,4)
       +.01*BINAND(B2,a5))
```

```
1060 Out(J)=DROUND(Out(J),6)
1070 NEXT I
1080 BEEP 330,.50
1090 !
1100 PRINT "The data conversion is complete."
1110 PRINT
1120 !
1130 INPUT "Do you want a hard or soft copy (H of S)",Ans$
1140 PRINT
1150 PRINT "Is there any interval you desire to see?"
1160 PRINT "Example: every 5th point set"
1170 PRINT "enter 1 for every data point, 5 for every 5th"
1180 PRINT
1190 PRINT "WARNING - THERE ARE 260 DATA SETS TOTAL"
1200 PRINT "THAT IS A LOT OF PAPER"
1210 PRINT
1220 PRINT "PRINTOUT IS IN GROUPOS OF 50"
1230 PRINT "TO PUNCHOUT ENTER '999'"
1240 PRINT
1250 BEEP
1260 INPUT 0
1270 If Q<=0 THEN Q=1
1280 IF Ans$="h" OR Ans$="H" THEN
1290  PRINTER IS 706
1300 ELSE
1310  PRINTER IS 1
1320 END IF
1330 PRINT
1340 PRINT
1341 Punch=0
1350 Fmt1: IMAGE DDDDD,5X,MDD.DDDD,5X,M.DDDDDDD
1360       PRINT "N","LOAD","DISP"
1370       PRINT
1380       FOR I=1 TO 250
1381 IF Punch<>999 THEN
1390  IF I/50=INT(I/50) THEN INPUT Punch
1400 END IF
1410!****Change the endng value above
1420      X(I)=(Out(2*I)-Disv)*Sf    !Displacement
1430 IF I>1 THEN X(I)=(X(I)+X(I-1)/2
1440      Y(I)=Out(2*I-1)*Lf    !Load
1450 IF I/Q=INT(I/Q) OR I=2 THEN
1460  IF Punch<>999 THEN PRINT USING Fmt1;I,Y(I),X(I)
1470  END IF
1480  NEXT I
1490 Dump;!
1500  PRINTER IS 1
1510  !
1520  INPUT "What is your FILENAME?",Name$
1530  PRINT
1540  PRINT "What range and frequency of points do you want
        to save"
```

```
1550   PRINT "'START,STOP,STEP'"
1560   PRINT
1570   INPUT St,Sp,Stp
1580   Siz=INT((Sp-St)/Stp)/15)
1590   CREATE BDAT Name$,Siz
1600   ASSIGN @Path TO Name$
1610   FOR J=St TO Sp STEP Stp
1620    OUTPUT @Path;Y(J)<X(J)
1630   NEXT J
1640   PRINT
1650   BEEP
1660    PRINT
1670    PRINT "The program is now complete"
1680    BEEP
1690    BEEP
1691  GOTO Compl
1693 Errcheck:!
1694    If ERRN=54 THEN
1695     PRINT "Duplicate FILENAME- TRY AGAIN"
1696     GOTO 1520
1697    END IF
1698 Compl:!
1700    END
```

APPENDIX B

AREA-CALCULATING PROGRAM FOR USE IN CONJUNCTION WITH THE F COLLECT DATA ACQUISITION PROGRAM

```
10   !*********************************
20  !This program will calculate a simple
30  !area under/between the curves for
40  !hysteresis loop data --- The input file
50  !should be in the form LOAD,DISPLACEMENT
60  !as stored by the data collection routine
70  !'COLLECT' or 'F_COLLECT'
80  !                                  11/5/87
90  !*********************************
100 ! Data retrieval portion
110 INPUT "What is your INPUT DAT FILE NAME",Dat$
120 PRINT
130 DIM Lod(350),Displ(350),Strs(350),Strn(350)
140 PRINT "Is your data disc in?"
150 PRINT "Press 'CONTINUE' when ready"
160 PAUSE
170 LO=.5
180 Pie=3.14159
190 PRINT
200 INPUT "What is our initial diameter",DO
210 PRINT
220 AO=(Pie/4)*DO^2
230 ASSIGN @Path1 TO Dat$
240 FOR N=1 TO 6000
250 ON END @Path1 GOTO 440
260 ENTER @Path1;Lod(N),Displ(N)
270  IF Max1<Lod(N) THEN
280    Max1=Lod(N)
290    Max1pt=N
300  END IF
310  IF Min1>Lod(N) THEN
320    Min1=Lod(N)
330    Min1pt=N
340  END IF
350  IF Maxd<Displ(N) THEN
360    Maxd=Displ(N)
370    Maxdpt=N
380  END IF
390  IF Mind>Displ(N) THEN
400    Mind=Displ(N)
410    Mindpt=N
420  END IF
430 NEXT N
```

```
440 M=N-2
450 ASSIGN @Path1 TO *
460 BEEP 300,1
470 PRINT M;" Data points have been read"
480 PRINT "Stresses and Strains Are now being calculated"
481 PRINT "PLEASE WAIT"
490 PRINT
500 !****************************************
510 !CALC OF TRUE STRESSES AND TRUE STRAINS"
520 !
530 FOR N=1 TO M
540  Li=LO+Displ(N)
550  Ai=(A0*L0)/Li !Based on const vol deformation
560  IF Li?LO THEN
570   Strn(N)=LOG(Li/L0)   ! In tension
580 ELSE
590   Strn(N)=LOG(L0/Li)   ! In compression
600  END IF
610   Strs(NJ)=Lod(N)/Ai
620 NEXT N
630 Area=0
640 Totang=0
650 Que=0
660 !****************************************
670 ! Area under the stress/strain curve calc
680 !
681 PRINT "The area of the loop is now being"
682 PRINT "calculated - PLEASE WAIT"
683 PRINT
690 FOR N=2 TO M
700   Ang1=ATN(Lod(N-1)/Displ(N-1))
710   Ang2=ATN(Lod(N)/Displ(N))
730  IF Totang<6.283185 THEN
740   Dstrn=Strn(N)-Strn(N-1)
750   Avgstra=(Strs(N)+Strs(N-1))/2
760   Area=Area+(Dstrn*Avgstrs)
770   Que=N    ! The last point for 1 full loop
780  END IF
790 NEXT N
800 ! Calc of the area fm last point to the start of loop
810 Dstrn=Strn(1)-Strn(Que)
820 Avgstrs=(Strs(1)+Strs(Que))/2
830 Area=Area+(Dstrn*Avgstrs)
840 !******************************
850 ! Printout part
860 !
870 PRINTER IS 706
880 PRINT
890 PRINT
900 PRINT "For the hysteresis loop of file ";Dat$
910 PRINT "The total area enclosed by the stress/strain is:"
920 PRINT Area;" ksi,in/in"
```

```
930 PRINT
940 PRINT
950 PRINT
951 PRINTER IS 1
960 END
```

APPENDIX C

TABULATED SDC AND FREQUENCY DATA

1. Specimen: Fe-Cr-Al, 900 C (See Figure 8)

Load: ± 400 lbs

FREQ (Hz)	SDC (%)
1-2.5	8.20
3.0	11.87
3.3	36.09
3.5	42.20
3.7	46.19
4.0	47.92
4.2	29.01
5.0	27.54
6.0	19.71
8.0	13.31

Load: ± 800 lbs

FREQ (Hz)	SDC (%)
1.0	3.96
1.5	12.28
1.8	33.57
2.0	46.92
2.3	51.45
2.5	48.93
2.9	13.16
4.0	10.63
6.0	9.84
8.0	6.60

Load: ± 1200 lbs

FREQ (Hz)	SDC (%)
1.0	3.63
1.5	15.05
1.8	53.07
2.0	64.36
2.5	56.51
3.0	45.88
4.0	26.79
6.0	17.94
8.0	10.89

Load: ± 1600 lbs

FREQ (Hz)	SDC (%)
1.0	6.44
1.3	19.46
1.5	41.76
1.8	56.44
2.0	48.18
2.5	39.68
3.0	32.03
5.0	12.63
7.0	10.00

Load: ± 2000 lbs

FREQ (Hz)	SDC (%)
0.5	2.14
1.0	11.87
1.2	13.84
1.5	45.09
1.8	38.35
2.5	39.61
3.0	21.94
5.0	11.94
7.0	8.04

2. Specimen: Fe-Cr-Al, 1100 C (See Figure 9)

Load: ±400 lbs

FREQ (Hz)	SDC (%)
1.0-2.5	6.47
3.0	13.23
3.2	30.28
3.5	48.31
3.8	49.90
4.0	50.31
5.0	15.74
8.0	16.22

Load: ± 800 lbs

FREQ (Hz)	SDC (%)
1.0	3.75
1.5	12.05
1.8	35.02
2.0	51.46
2.5	55.46
2.8	51.32
3.0	17.75
4.0	9.94
8.0	8.08

Load: ± 1200 lbs

FREQ (Hz)	SDC (%)
1.0	4.2
1.5	11.07
1.8	19.87
2.0	55.51
2.2	62.24
2.5	54.01
3.0	47.09
4.0	31.69
6.0	18.18
8.0	13.15

Load: ± 1600 lbs

FREQ (Hz)	SDC (%)
1.0	5.02
1.5	14.71
1.6	42.14
1.8	52.58
2.0	43.66
2.5	42.58
3.0	32.94
4.0	32.94
6.0	12.78
8.0	7.90

Load: ±2000 lbs

FREQ (Hz)	SDC (%)
1.0	6.36
1.2	29.03
1.4	35.22
1.5	40.94
1.7	35.65

FREQ (Hz)	SDC (%)
2.0	30.97
3.0	20.00
4.0	13.42
6.0	8.31
8.0	5.38

3. Specimen: Fe-Cr-Mo, 900 C (See Figure 10)

Load: ± 400 lbs

FREQ (Hz)	SDC (%)
1-2.5	5.76
3.0	12.73
3.5	46.31
4.0	50.28
4.5	17.41
5.0	9.56
6.0	14.21
8.0	3.35

Load: ± 800 lbs

FREQ (Hz)	SDC (%)
1.0	4.13
1.5	12.11
1.8	35.07
2.0	48.77
2.5	54.22
3.0	30.60
3.5	10.58
4.0	7.16

Load: ± 1200 lbs

FREQ (Hz)	SDC (%)
1.0	3.20
1.5	4.74
1.9	32.48
2.0	44.00
3.0	44.98
3.5	33.70
4.0	28.83
6.0	15.83
8.0	10.70

Load: ± 1600 lbs

FREQ (Hz)	SDC (%)
1.0	2.84
1.5	4.99
1.7	47.88
2.0	40.85
2.5	31.75
3.0	23.32
4.0	18.95
6.0	13.55
8.0	12.46

Load: ± 2000 lbs

FREQ (Hz)	SDC (%)
1.0	4.33
1.3	5.42
1.4	37.42
1.5	35.68
1.7	31.59
2.0	31.62
3.0	19.72
5.0	11.07
8.0	5.74

4. Specimen: Fe-Cr-Mo, 1100 C (See Figure 11)

Load: ± 400 lbs

FREQ (Hz)	SDC (%)
1.0-2.5	4.40
3.0	12.30
3.2	29.20
3.5	48.54
3.7	50.88
4.0	53.25
4.2	55.06
5.0	16.75
6.0	17.08
8.0	16.06
10.0	13.71

Load: ± 800 lbs

FREQ (Hz)	SDC (%)
1.0	4.16
1.5	10.72
2.0	48.52
2.2	54.30
2.5	55.04
2.7	52.68
2.8	38.59
3.0	14.63
4.0	12.69
6.0	10.04
8.0	7.66
10.0	7.01

Load: ± 1200 lbs

FREQ (Hz)	SDC (%)
1.0	4.02
1.5	12.28
1.8	22.57
2.0	62.80
2.2	65.32
2.5	59.38
3.0	46.82
4.0	33.23

Load: ± 1600 lbs

FREQ (Hz)	SDC (%)
1.0	4.62
1.2	11.20
1.5	42.84
1.7	56.47
1.8	56.22
2.0	33.60
2.5	36.73
3.0	26.42
4.0	23.21
6.0	12.00

Load: ± 2000 lbs

FREQ (Hz)	SDC (%)
0.5	2.19
1.0	10.46
1.3	48.78
1.5	46.84
1.8	34.10
2.0	31.35
3.0	20.55
4.0	15.44
6.0	9.00

LIST OF REFERENCES

1. Schetky, L.M. and Perkins, J., "The 'Quiet' Alloys," Machine Design, pp. 202-206, 6 April 1978.

2. Perkins, J., Edwards, G.R. and Hills, N., "Materials Approaches to Ship Silencing," Report, U.S. Naval Postgraduate School, June 1974.

3. Bert, C.W., "Material Damping: An Introductory Review of Mathematical Models, Measures, and Experimental Techniques," Journal of Sound and Vibration, Vol. 29, No. 2, pp. 129-153, 1973.

4. Kawabe, H. and Kuwahara, K., "A Consideration of the Strain Amplitude-Dependent Damping and Modulus in Ferromagnetic Metals," Transactions of the Japan Institute of Metals, Vol. 22, No. 5, pp. 301-308, 1981.

5. Masumoto, H., Hinai, M. and Sawaya, S., "Damping Capacity and Pitting Corrosion Resistance of Fe-Mo-Cr Alloys," Transactions of the Japan Institute of Metals, Vol. 25, No. 12, pp. 891-899, 1984

6. Willertz, L., "Magnetomechanical Damping Properties of AISI 403 Stainless Steel with Applied Static Torsional and Axial Stesses," Journal of Testing and Evaluation, JTEVA, Vol. 2, No. 6, pp. 478-482, November 1974.

7. Bolt, Beranek and Newman, Inc., Cambridge, Massachusetts, Operations Manual for the Bolt, Beranek and Newman, Inc., Resonant Dwell Apparatus, January 1973.

8. O'Toole, J.F., Damping Behavior of an Fe-Ce-Mo Alloy: Strain Dependent and Heat Treatment Effects, M.S. Thesis, Naval Postgraduate School, Monterey, California, December 1986.

9. Ferguson, D., Characterization of High Damping Fe-Cr-Mo and Fe-Cr-Al Alloys for Naval Ships Application, M.S. Thesis, Naval Postgraduate School, Monterey, California, March 1988.

10. Cronauer, J., Damping Behavior of a Ni-Ti Shape Memory Alloy: Comparison with Cu-Mn-Based and Fe-Cr-Based High Damping Alloys, M.S. Thesis, Naval Postgraduate School, Monterey, California, June 1987.

11. Patch, G., Development of a Data Acquisition and Analysis System for High Damping Alloy Evaluation, M.S. Thesis, Naval Postgraduate School, Monterey, California, September 1987.

12. Suzuki, K., Fijita, T. and Haseb, M., "Damping Capacity and Mechanical Properties of Sintered Fe-Cr-Mo High Damping Alloy," Powder Metallurgy, No. 4, pp. 409-413, 1970.

13. Escue, W.D., Characterization of the Corrosion Behavior of High Damping Alloys in Seawater, M.S. Thesis, Naval Postgraduate School, Monterey, California, June 1987.

14. Ahktar, S. and Kellogg, T.F., Corrosion Behavior of High Damping Alloys in 3.5% NaCl Solution, M.S. Thesis, Naval Postgraduate School, Monterey, California, September 1987.

15. Laboratory Certificate of Chemical Analysis performed by Anamet Laboratories, Inc., May 1987.

16. Naval Underwater Systems Center Report TD 6927, "A Technical Update on Damped Vacrosil-010," by R.G. Kasper, September 1983.

17. Schneider, W., Schrey, P., Hausch, G. and Torok, E., "Damping Capacity of Fe-Cr and Fe-Cr Based High Damping Alloys," Journal De Physique, Colloque C5, Supplement au n 10, Tome 42, pp. C5-C35, October 1981.

18. de Batist, R., "High Damping Materials: Mechanisms and Applications," Journal de Physique, Vol. 44, pp. C9-39--C9-50, December 1983.

19. Cochardt, A., "The Origin of Damping in High-Strength Ferromagnetic Alloys," Transactions of the ASME, Vol. 75, pp. 196-200, 1953.

20. Nashif, A., Jones, D. and Henderson, L., Vibration Damping, John Wiley and Sons, 1985.

21. Ray, A., Wren, G. and Kinra, V., "Comparison of Experimental Techniques in the Measurement of Damping Capacity of Metal-Matrix Composites," Paper presented at the Eleventh Biennial Conference on Mechanical Vibrations and Noise of the ASME, September 1987.

INITIAL DISTRIBUTION LIST

		No. Copies
1.	Defense Technical Information Center Cameron Station Alexandria, Virginia 22304-6145	2
2.	Library, Code 0142 Naval Postgraduate School Monterey, California 93943-5002	2
3.	Professor Jeff Perkins, Code 69 Ps Department of Mechanical Engineering Naval Postgraduate School Monterey, California 93943-5004	3
4.	LT James L. Childs Superintendent of Shipbuilding San Francisco, California 94124-2996	3
5.	Mrs. Catherine Wong, Code 2812 David Taylor Naval Ship R & D Center Annapolis, Maryland 21402	3
6.	Mr. Robert Hardy, Code 2803 David Taylor Naval Ship R & D Center Annapolis, Maryland 21402	3
7.	Dean of Science and Engineering, Code 06 Naval Postgraduate School Monterey, California 93943-5000	1
8.	Research Administration, Code 012 Naval Postgraduate School Monterey, California 93943-5000	1
9.	Department Chairman, Code 69Hy Department of Mechanical Engineering Naval Postgraduate School Monterey, California 93943-5004	1
10.	Professor Y. S. Shin, Code 69Sg Department of Mechanical Engineering Naval Postgraduate School Monterey, California 93943-5000	1

11. Mr. Charles Zanis, Code 196 — 1
Naval Sea Systems Command
Washington, D.C. 20362-5101

12. LCDR Wallace M. Elger, Code 05MB — 1
Naval Sea Systems Command
Washington, D.C. 20362-5101

13. Mr. A. G. S. Morton, Code 2813 — 1
David Taylor Naval Ship R & D Center
Annapolis, Maryland 21402

14. Mr. V. J. Castelli, Code 2844 — 1
David Taylor Naval R & D Center
Annapolis, Maryland 21402